SUBSET SIMULATION FOR RELIABILITY ESTIMATION OF MECHANICAL COMPONENTS SUBJECTED TO FATIGUE USING THE FORMAN-METTU MODEL

A. Altamura, *Tenaris, Research & Development, Italy & Technische Universität München*
D. Straub, *Technische Universität München, Engineering Risk Analysis Group, Germany*

ABSTRACT

In this work, an advanced reliability evaluation method is implemented in conjunction with a state of the art fatigue crack growth evaluation, to determine the fatigue reliability under variable amplitude loading. Material properties and initial crack geometry are modelled as random variables, based on experimental observations. Fatigue loads are treated as a random process, characterised by varying correlation lengths. A crack growth algorithm is implemented using an approximated integration of the Forman-Mettu equation, also known as Nasgro equation, which accounts for the fatigue threshold and describes well the three regions of the fatigue crack growth curve. The subset simulation method is presented and applied to compute the reliability of mechanical components subject to internal pressure fatigue loads. In the numerical investigations, it is found that the assumptions on the correlation length of the load process have significant influence on the resulting reliability; the probability of failure can vary up to several orders of magnitude. This points to the importance of an accurate modelling of the fatigue load processes.

NOMENCLATURE

a crack depth
a_0 initial crack depth
c crack semi-length
f Newman's closure function
f' prior probability distribution
f'', f(a|ND) posterior probability distribution
f_a fatigue crack growth rate in a-direction
f_c fatigue crack growth rate in c-direction
f_x fatigue crack growth rate
$g(X)$, $g(U)$ limit state function
k_0, k, k_{min} parameters of the toughness distribution
m, p, q, C, C_{th}, A_0 Forman-Mettu equation parameters
p_F probability of failure
x crack length
X vector of random variables
U vector of standard normal uncorrelated random variables
V vector of standard normal correlated random variables
z correlation length of the load distribution
CDF cumulative density function
$CDFF$ crack driving force failure
E elastic modulus
F cumulative density function
F_y yield load
J J-integral
J_e elastic J-integral
J_{mat} fracture toughness expressed as J-integral
K stress intensity factor
K_{mat} fracture toughness expressed as K-factor
K_{max} maximum stress intensity factor
L length of the tubes
L_r ligament yielding factor
N number of cycles
N_{Fail} number of cycles at failure
N_{target} target number of cycles
N_{stop} number of cycles at which the crack growth algorithm stops
NDT non-destructive tests
P load
POD probability of detection
Q material properties dependant parameter in the formulation of L_r
R stress ratio
R_{el} elastic limit
UTS ultimate tensile strength
WT wall thickness
β boundary correction factor

θ, ζ parameters of the POD distribution
ν Poisson's ratio
σ_y yield strength
$\sigma_{y,cycl}$ cyclic yield strength
ρ geometric parameter in the formulation of L_r
ΔK stress intensity factor range
ΔK_{th} fatigue threshold
ΔK_{th0} fatigue threshold at $R = 0$
$\Delta\sigma$ stress range
Φ standard normal cumulative density function

1. INTRODUCTION

The assessment of the fatigue life of mechanical components subjected to variable amplitude loads can be addressed with various approaches. The standards EN13445 [1] and Eurocode 3 [2] use damage accumulation rules and provide relevant $S-N$ curves taken from experimental data. Alternatively a crack growth evaluation can be carried out, applying the simple Paris equation, as recommended in BS7910 [3], a bilinear curve or the Forman-Mettu equation [4], which describes the entire crack growth behaviour from the threshold region to the failure zone.
Due to the variability of the applied loads and to the uncertainty of many input variables, such as the presence of initial flaws or the fatigue resistance of the material, a probabilistic approach is required to avoid over-conservative results and to achieve an optimized design.
Many crack propagation stochastic models have been developed, such as those proposed in [5] and [6]. A first-order approximation can be used to rapidly estimate the expected value of the fatigue life, [7], but the evaluation of the full distribution of the fatigue lifetime requires more complex approaches.
To model variable amplitude loading, many standardized load sequences have been proposed [8], but their repetition introduces sequence effects [9]. Variable amplitude load sequences can be better described as random processes [10, 11, 12,13].
This paper exemplarily addresses tubes for hydraulic cylinders subjected to internal pressure fatigue loading. In this work an advanced method to efficiently evaluate the reliability, namely the subset simulation [14], is applied in combination with a cumulative integration of the Forman-Mettu equation, also known as Nasgro equation [4, 14]. The description of the loads as random processes with varying correlation length provides insights into the influence of the load sequence on the reliability.

2. CRACK GROWTH

2.1 MECHANICAL MODEL

Hydraulic cylinders are subjected to internal pressure fatigue loads. This type of loading causes hoop stresses, which are here considered to be constant through the tube wall. Surface flaws might be present on the tube surface, from which fatigue crack growth can initiate.
Experimental observations on surface flaws in such components are reported in [16 - 18]. The geometry of these flaws can be modelled by a semi-elliptical shape that is characterized by a depth *a* and a semi-length *c*. Under fatigue loading, the crack grows in both directions *a* and *c*, as shown in Fig. (1).

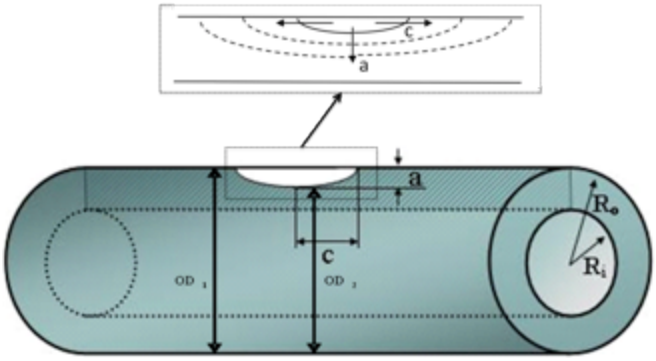

Fig. 1. Scheme of a tube having a semi-elliptical surface flaw characterized by the depth *a* and the semi-length c.

2.2 CRACK GROWTH

Crack growth in the two directions is modelled by the following coupled differential equations as a function of a, c, stress range $\Delta\sigma$ and stress ratio R:

$$\frac{da}{dN} = f_a(a, c, \Delta\sigma, R) \quad (1a)$$

$$\frac{dc}{dN} = f_c(a, c, \Delta\sigma, R) \quad (1b)$$

The crack growth rates $f_x(a, c, \Delta\sigma, R)$ in both directions a or c are described by the Forman-Mettu equation:

$$f_x(a, c, \Delta\sigma, R) = C\left[\left(\frac{1 - f(\Delta\sigma, R)}{1 - R}\right)\Delta K_x(a, c, \Delta\sigma, R)\right]^m \cdot \frac{\left(1 - \frac{\Delta K_{th}(\Delta\sigma, R)}{\Delta K_x(a, c, \Delta\sigma, R)}\right)^p}{\left(1 - \frac{K_{x,max}(a, c, \Delta\sigma, R)}{K_{mat}}\right)^q} \quad (2a)$$

$$\Delta K_{th}(\Delta\sigma, R) = \frac{\Delta K_{th,0}}{\left[\frac{1 - f(\Delta\sigma, R)}{[1 - A_0(\Delta\sigma, R)](1 - R)}\right]^{(1 - C_{th}R)}} \quad (2b)$$

Here, x is the crack dimension (either a or c), p, q, m, C and C_{th} are empirical parameters obtained from the fitting to experimental data. ΔK_x is the stress intensity factor range in x-direction. The stress ratio R is assumed constant and equal to *0.1*. $K_{max,x}$ is the maximum stress intensity factor in x-direction, given as:

$$K_{max,x}(a, c, \Delta\sigma, R) = \frac{\Delta K_x(a, c, \Delta\sigma)}{1 - R} \quad (3)$$

K_{mat} is the material fracture toughness and $f(R)$ denotes the Newman's crack opening function [19] which is defined as the ratio of the opening stress and the maximum applied stress, $\frac{\sigma_0}{\sigma_{max}}$. ΔK_{th} is the fatigue threshold, computed as a function of $\Delta K_{th,0}$, the fatigue threshold at a reference level of $R = 0$. A_0 is a function of the three-dimensional constraint and of the ratio of the maximum applied stress to the yield stress, $\frac{\sigma_{max}}{\sigma_y}$.

The stress intensity factor range ΔK_x is obtained according to eq. (4), based on the solution for a semi-elliptical surface flaw on a plate subjected to pure tension [20, 21]. This solution applies to thin wall thickness pipes, in which the hoop stresses can be considered constant through the wall.

$$\Delta K_x(a, c, \Delta\sigma) = \beta_x\left(\frac{a}{c}, \frac{a}{WT}, \frac{c}{L}\right)\Delta\sigma\sqrt{\pi a} \quad (4)$$

The boundary correction factor β_x is obtained according to the stress intensity solution for a semi-elliptical surface crack in a flat plane with $a \leq c$ [20, 21].

Assuming that the ratio $\frac{a}{c}$ is constant, Eqs. (1a) and (1b) can be written as:

$$dN = \frac{dx}{f_x(x, \frac{a}{c}, \Delta\sigma, R)} \quad (5)$$

If additionally $\Delta\sigma$ is assumed constant, Eq. (5) can be integrated on both sides to obtain:

$$\int_N^{N+\Delta N} dN = \Delta N = \int_x^{x+\Delta x} \frac{dx}{f_x\left(x, \frac{a}{c}, \Delta\sigma, R\right)}. \quad (6)$$

The right-hand side of this equation can be numerically integrated to evaluate the number of cycles ΔN necessary for the crack to grow from x to $x + \Delta x$.

However, because $\frac{a}{c}$ is not a constant and variable amplitude loads are present, Eq. (6) does not hold. The applied bi-dimensional crack-growth model implies that the crack growth in directions a and c cannot be evaluated separately, since the value of the boundary correction factor β_x depends on the ratio $\frac{a}{c}$. Furthermore, under variable amplitude loading, $\Delta\sigma$ varies with time and, therefore, is a function of N, i.e. $\Delta\sigma(N)$. It follows that the integrations over N and over x cannot be performed separately.

To evaluate the crack growth exactly, it is necessary to cumulatively calculate the crack increment Δx for every stress cycle. Given the large number of stress cycles, such an approach, however, is not computationally feasible. Therefore, the integration of Eqs. (1a) and (1b) is performed by dividing the cycles into blocks of ΔN cycles. In each block k, comprising the cycles from N_i to $N_i + \Delta N$, the stress range $\Delta\sigma$ is assumed to be constant and equal to the value at $N_i + \frac{\Delta N}{2}$ cycles (corresponding to the midpoint discretization). Additionally, the boundary correction factor β_x is also approximated by a constant value, equal to value at N_i cycles, i.e. at the beginning of the block. Under these assumptions, Eq. (5) holds and is applied to compute the crack size increment Δx in the ith block. Δx is found through a root finding algorithm, by numerically evaluating the integral

in Eq. (6) for various values of Δx and finding the one corresponding to ΔN.

2.3 INITIAL FLAW SIZE

The tubes are subjected to a quality control by means of non-destructive testing, to identify and eliminate detected surfaces flaws. Therefore, when modelling the probability distribution of the size of the initial surface flaws, the probability of detection (POD) of the applied non-destructive tests must be taken into account. Here, the POD is modelled by a lognormal cumulative distribution function [22] depending on the initial crack depth a_0:

$$POD(a_0) = \Phi\left(\frac{\ln(a_0) - \theta}{\zeta}\right) \qquad (7)$$

According to Bayes' rule, the posterior probability density function of surface flaws given the event of no detection $f(a_0|ND)$ is computed as:

$$f''(a_0) = f(a_0|ND) = \frac{f'(a_0)[1 - POD(a_0)]}{\int_0^\infty f'(a_0)[1 - POD(a_0)]da_0} \qquad (8)$$

Where $f'(a_0)$ is the prior probability density function (PDF) of the flaw depth before the NDT tests. Figs. 2a and 2b show the prior PDF $f'(a_0)$, the posterior PDF $f''(a_0)$ and $POD(a_0)$, for two different $PODs$, corresponding to two different levels of quality control.

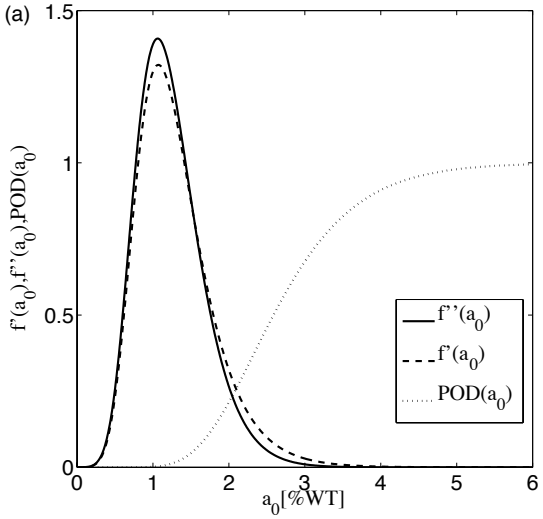

Fig. 2a Updating the initial flaw size distribution following quality control, where a is expressed as a percentage of the tube wall thickness and the mean threshold of NDT is equal to 2.7% of the tube wall thickness.

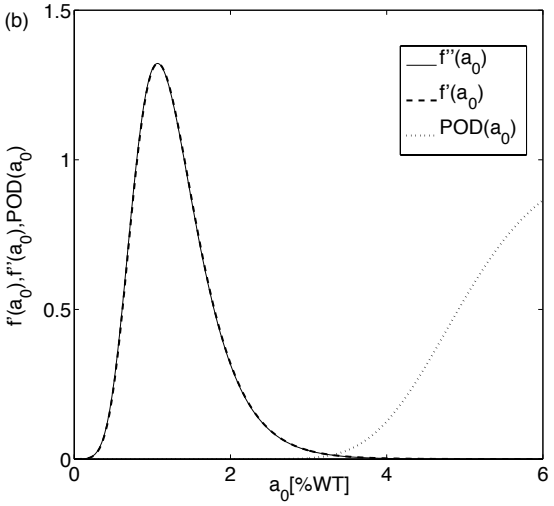

Fig. 2b Updating the initial flaw size distribution following quality control, where a is expressed as a percentage of the tube wall thickness and the mean threshold of NDT is equal to 5% of the tube wall thickness.

2.4 FAILURE CRITERIA

Two failure criteria are relevant:

- *Leakage*: stable crack growth until the crack depth reaches the tube wall thickness. Failure is modelled as the event of the crack depth exceeding 95% of the wall thickness.
- *Crack driving force failure condition* ($CDFF$): the applied crack driving force exceeds the fracture resistance of the material, which accounts for both plastic collapse and unstable crack growth.

The $CDFF$ assessment is carried out according to the procedure in [23]. The analytical solution for a tension loaded flat plane, valid for materials not displaying a yield plateau, are used.

To check for plastic collapse, the ligament yielding factor L_r is evaluated as:

$$L_r = \frac{\sigma_{ref}}{\sigma_y} = \frac{\sigma_m}{(1-\rho)\sigma_y} \qquad (9)$$

where σ_{ref} is the reference stress ($\sigma_{ref} = (\frac{P}{F_y}\sigma_y)$ where P indicates the load and $F_y$the yield load), σ_y is the yield stress, ρ is a geometric factor and σ_m is the membrane stress. Plastic collapse occurs when $L_r \geq L_{rmax}$, with L_{rmax} being the plastic collapse limit.

To check for unstable crack growth, the J-integral is evaluated as:

$$J_{applied} = J_e \cdot f(L_r)^{-2} \quad (10a)$$

$$J_e = \left(\frac{K_{a,max}{}^2}{E(1-\upsilon^2)}\right) \quad (10b)$$

where $K_{a,max}$ is determined following Eq. (3), E is Young's Modulus and ν is the Poisson ratio. The function $f(L_r)$ is defined as:

$$f(L_r) = \begin{cases} \dfrac{[0.3 + 0.7\exp(-\mu L_r^6)]}{(1+0.5L_r^2)^{0.5}}, & 0 \le L_r \le 1 \\ f(L_r = 1)L_r^{2Q}, & 1 < L_r \le L_{r,max} \end{cases} \quad (11)$$

where the parameters μ, Q, depend on the material and the geometry following the relations given in [23].

Unstable crack growth occurs when $J \geq J_{mat}$. The material fracture toughness expressed in terms of the *J-integral*, J_{mat}, is a function of the material fracture toughness expressed as *K-factor*, K_{mat}:

$$J_{mat} = \frac{K_{mat}^2}{E(1-\nu^2)} \quad (12)$$

Fig. (3) illustrates the different cases that can be encountered when evaluating crack growth: no propagation, propagation without failure, failure by leakage or by $CDFF$ condition.

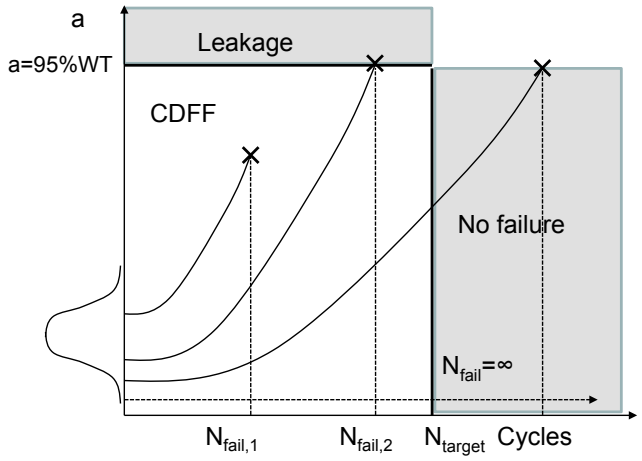

Fig. 3. Illustration of crack growth and the possible failure modes. Failure by $CDFF$ or by leakage can occur, in this example, at $N_{Fail,1}$ and at $N_{Fail,2}$, respectively. Any case when $N_{Fail} > N_{target}$ is in the "No Failure" domain and when no propagation occurs N_{Fail} is equal to infinite.

2.5 LIMIT STATE FUNCTION FOR FATIGUE FAILURE

The fatigue failure event can be described by the single limit state function:

$$g(\mathbf{X}) = N_{Fail}(\mathbf{X}) - N_{target} \quad (13)$$

where N_{target} is the number of stress cycles during the anticipated service life time and $N_{Fail}(\mathbf{X})$ is the number of cycles to failure as a function of the random variables $\mathbf{X}$, as illustrated in Fig. (3). This limit state function includes both the leakage failure and the *CDFF* criterion. The computation of $N_{Fail}(\mathbf{X})$ is summarized in the flow chart in Fig. (4). To avoid long computations, the evaluation of the crack growth stops at N_{stop} cycles. N_{stop} is a number larger than N_{target} that is selected according to the algorithm used for reliability analysis.

3. FATIGUE STRESSES AS A RANDOM PROCESS

3.1 CONSTANT AND VARIABLE AMPLITUDE LOADING

It can be distinguished between constant amplitude loading and variable amplitude loading.

In the case of constant amplitude loading (with constant stress ratio R), two situations can be encountered in the presence of initial flaws. If the applied stress intensity factor is higher than the threshold, the crack propagates and the failure condition is typically reached after a relatively short number of cycles. If the stress intensity factor is below the fatigue threshold, the crack does not propagate. In the case of constant amplitude loading, the stress ranges can be modelled by a random variable or a deterministic parameter.

When variable amplitude loading is applied, generally a fraction of the applied stress cycles leads to crack propagation whereas the remaining cycles are below the fatigue threshold. In this case the applied stress ranges should ideally be modelled by a random process. Such a model is presented in the following section.

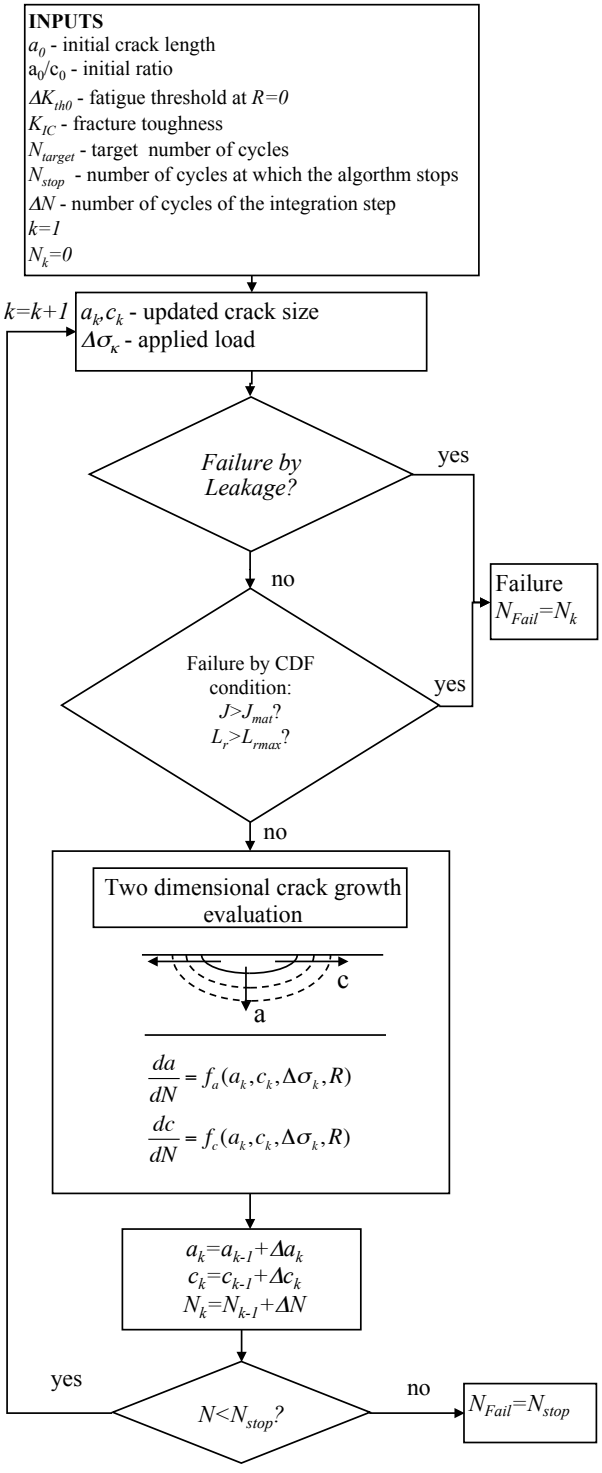

Fig. 4. Algorithm for evaluating N_{Fail}.

3.2 RANDOM PROCESS MODELLING OF FATIGUE LOADS

In this work, the applied load is described as a stationary random process $\{\Delta\sigma(N)\}$ with cumulative distribution function (CDF) $F_\pi(\pi(N))$. The joint distribution of any two stress ranges $\Delta\sigma(N_i)$ and $\Delta\sigma(N_j)$ is described by a Gaussian copula, which is outlined in the following.

Let $\Delta\sigma(N_i)$ be defined through a transformation T from a standard Normal variate $V(N_i)$ as:

$$\Delta\sigma(N_i) = T(V_i) = F_{\Delta\sigma}^{-1}[\Phi(V(N_i))] \qquad (14)$$

where Φ is the standard Normal CDF and $F_{\Delta\sigma}^{-1}$ is the inverse of the CDF of $\Delta\sigma(N_i)$. If it is imposed that $V(N_i)$ and $V(N_j)$ have the joint Normal distribution, then the $\Delta\sigma(N_i)$ and $\Delta\sigma(N_j)$ defined through the transformation in Eq. (14) are said to follow the Gaussian copula, also known as Nataf distribution.

The autocovariance function of the process $\{\Delta\sigma(N)\}$ is described through an autocovariance function of the underlying standard Normal process $\{V(N)\}$:

$$Cov[V(N_i), V(N_j)] = exp\left(-\frac{N_i - N_j}{z}\right) \qquad (15)$$

where z is the correlation length.

It can be shown that with this autocovariance function, the process $\{V(N)\}$ has the Markovian property [24]. Consequently, the process $\{\Delta\sigma(N)\}$ is a Markov process, i.e.

$$F_v[v(t_n)|v(t_{n-1}), v(t_{n-2}), .. v(t_1)] = F_v[v(t_n)|(t_{n-1})] \qquad (16)$$

3.3 APPROXIMATION OF THE LOAD SEQUENCE

As explained in Section 2.2, the evaluation of the crack growth is carried out by approximating the fatigue load by blocks of length ΔN with constant stress amplitudes. The stress range process is therefore represented by $l = \frac{N_{stop}}{\Delta N}$ random variables $\Delta\sigma_k$, which are equal to the mid-point value of each block, i.e. $\Delta\sigma_k = \Delta\sigma\left(N_{k-1} + \frac{\Delta N}{2}\right)$. The approximate load sequence is illustrated in Fig. (5).

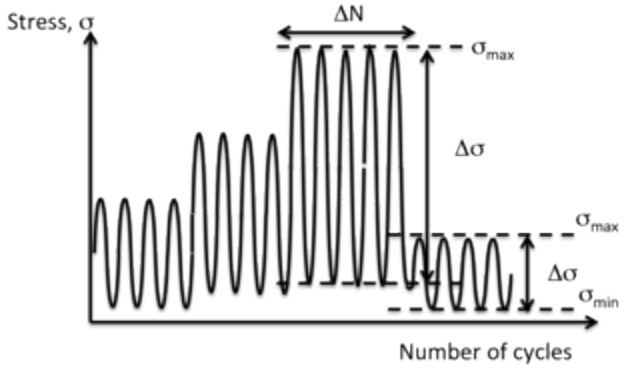

Fig. 5 Illustration of the simplified load sequence built as blocks of constant amplitude loads of length *ΔN*. The value of the stress amplitude in each block is equal to value of the original random process of the stress amplitude in the mid-point of each block.

3.4 ROSENBLATT TRANSFORMATION OF THE LOAD PROCESS

For reliability analysis, a transformation of uncorrelated standard Normal random variables $U_1, \dots, U_l$ to the discrete load process $\Delta\sigma_1, \dots, \Delta\sigma_l$ is required. The Markovian property of the process $\Delta\sigma_1, \dots, \Delta\sigma_l$ (see Eq. 16), facilitates the application of the Rosenblatt transformation [25 - 26] for this purpose. First, the random variables $U_1, \dots, U_l$ are transformed into the correlated standard normal random variables $V_1, \dots, V_l$ sequentially:

$$V_1 = F_{V_1}^{-1}\big(\Phi(U_1)\big) = U_1 \tag{17a}$$

$$V_2 = F_{V_2}^{-1}(\Phi(U_2)|V_1) = \frac{U_2 - \mu_{V_2|V_1}}{\sigma_{V_2|V_1}} \tag{17b}$$

$$V_3 = F_{V_3}^{-1}(\Phi(U_3)|V_2, V_1) = F_{V_3}^{-1}(\Phi(U_3)|V_2) = \frac{U_3 - \mu_{V_3|V_2}}{\sigma_{V_3|V_2}} \tag{17c}$$

$$\vdots$$

$$V_k = \frac{U_k - \mu_{V_k|V_{k-1}}}{\sigma_{V_k|V_{k-1}}} \tag{17d}$$

The conditional mean and standard deviation of V_k given V_{k-1} are:

$$\mu_{V_k|V_{k-1}} = V_{k-1}\rho \tag{18a}$$

$$\sigma_{V_k|V_{k-1}} = \sqrt{1-\rho^2} \tag{18b}$$

where the correlation coefficient ρ is equal to the covariance between V_{k-1} and V_k, defined following Eq. (15). Due to the stationarity of the load process, ρ is equal for all k.

Finally, $\Delta\sigma_1, \dots, \Delta\sigma_l$ are obtained from $V_1, \dots, V_l$ through the marginal transformation $T(V_k)$ defined in Eq. (14).

3.5 SOME OBSERVATIONS ON THE LOAD MODEL

It is worth noticing that the process $\{\Delta\sigma(N)\}$ does not have the same correlation function as the underlying Gaussian process $\{\mathrm{V}(N)\}$. However, the difference between $\mathrm{Cov}\big[\Delta\sigma(N_i), \Delta\sigma(N_j)\big]$ and $\mathrm{Cov}\big[V(N_i), V(N_j)\big]$ is generally small.

Because of the grouping of stress cycles into blocks of equal stress ranges (Section 3.3), the correlation among stress cycles is – on average – overestimated by the model, since this model implies a correlation of one among stress cycles within a block. The overestimation is relevant when the correlation length is equal to or smaller than ΔN.

4 SUBSET SIMULATION ALGORITHM

The subset simulation algorithm [14] is implemented to evaluate the probability of failure with respect to the limit state function defined in Eq. (13). This method permits to efficiently evaluate low probabilities of failure in problems involving a large number of random variables.

To facilitate the implementation, the limit state function is transformed from the space of the original random variables $\mathbf{X}$ to the space of uncorrelated standard Normal random variables $\mathbf{U}$. Let T denote the transformation of $\mathbf{X}$ to $\mathbf{U}$, $\mathbf{X} = T(\mathbf{U})$. For the discrete load process $\Delta\sigma_1, \dots, \Delta\sigma_l$, this transformation is described in Section 3.4; for the remaining random variables, only a marginal transformation is required. The limit state function in standard normal space $G(\mathbf{U})$ is:

$$G(\mathbf{U}) = g(T(\mathbf{U})) = N_{fail}\big(T(\mathbf{U})\big) - N_{target} \tag{19}$$

The failure event is correspondingly defined as:

$$Fail = \{G(\mathbf{U}) \leq 0\} \quad (20)$$

In subset simulation, intermediate failure events $E_i = \{G(U) \leq b_i\}, i = 1, \ldots, B$, are defined. It is $b_1 > b_2 > \cdots > b_B = 0$ and therefore $E_1 \supset E_2 \supset \ldots \supset E_B = Fail$. Because E_i is a subset of E_{i-1}, which in turn is a subset of E_{i-2} and so on, the probability of failure can be expressed as:

$$\begin{aligned} p_F &= P\left(\bigcap_{i=1}^{B} E_i\right) \\ &= P(E_B|E_{B-1})P\left(\bigcap_{i=1}^{B-1} E_i\right) \\ &= P(E_1)\prod_{i=2}^{B} P(E_i|E_{i-1}) \end{aligned} \quad (21)$$

where $P(E_i|E_{i-i})$ is the conditional probability of E_i given E_{i-1}.

The conditional probabilities $P(E_i|E_{i-i})$ are obtained by means of a Markov Chain Monte Carlo ($MCMC$) sampling approach using the modified Metropolis-Hastings ($M-H$) algorithm from [14]. This algorithm allows to generate samples from the conditional distribution of $\mathbf{U}$ given E_{i-1}, $F(\mathbf{U}|E_{i-1})$. The conditional probability $P(E_i|E_{i-1})$ is then evaluated from these samples using a Monte Carlo approach.

In this work, the constants b_i defining the intermediate failure events are chosen such that $P(E_i|E_{i-1}) = 10^{-1}$, and 500 samples are generated at each step.

5 CASE STUDY AND RESULTS

5.1 CASE STUDY

The case study is on tubular mechanical components subjected to internal pressure fatigue loads, as illustrated in Fig. 1. Crack growth and failure are modelled following Section 2.

Table 1 summarizes the material properties (mechanical characteristics and and parameters of the crack growth curve). These have been fitted to experimental data [16].

Table 1 Material properties

Parameter	Distribution	Value
K_{mat}	3-parameter Weibull $F(K_{mat}) = 1 - e^{\left\{-\left[\frac{K_{mat}-K_{min}}{(K_0-K_{min})}\right]^k\right\}}$	K_0= 40 MPa√m, k=5 K_{min}=28.7 MPa√m,
σ_y	-	590 MPa
$\sigma_{y,cycl}$	-	350 MPa
E	-	210.000 MPa
n	-	0.3
$\Delta K_{th,0}$	Gaussian	mean=5.5 MPa√m, stand. dev.=0.17
C_{th}	-	0.48
C	-	1.33 10-11 $MPa\sqrt{m}$ given $\frac{da}{dN}$ in $\frac{mm}{cycle}$
m	-	2.85
p	-	0.3
q	-	0.01

The correctness of the crack growth algorithm has been verified using:

- the commercial software AFGROW [15], wherein the Forman-Mettu equation is used to evaluate the growth of a centre semi-elliptical surface crack subjected to pure tension stress;
- full scale experimental data on tubes with artificial notches of 0.3 mm depth and 3 mm total length [16].

Table 2 shows the input parameters used for the case studies, namely the geometry of the tubes, the parameters of the applied POD curves, the initial ratio of $\frac{a}{c}$, the value of the stress ratio and of the anticipated number of cycles during service life, N_{target}. This number of cycles corresponds to a service life of 20000 hours.

Table 2 Input parameters

Parameter	Distribution	Value
Tube dimensions $OD\ x\ WT$	-	242 x 22 mm
initial flaw depth, a_0	Gumbel type I distribution	see Fig. 2
$POD(a_0)$	Lognormal CDF (eq. 7)	$\zeta = 0.32\ \theta = -0.56$ (Fig. 2a) $\zeta = 0.18\ \theta = 0.08$ (Fig. 2a)
$\frac{a_0}{c_0}$	-	0.1
R	-	0.1
N_{target}	-	$18 \cdot 10^6$

The model of the stress amplitude is derived from experimental measurements of load on hydraulic cylinders of earth moving machines [16]. The resulting empirical cumulative density function is shown in Fig. (6). Only stress amplitudes larger than 10 MPa are considered.

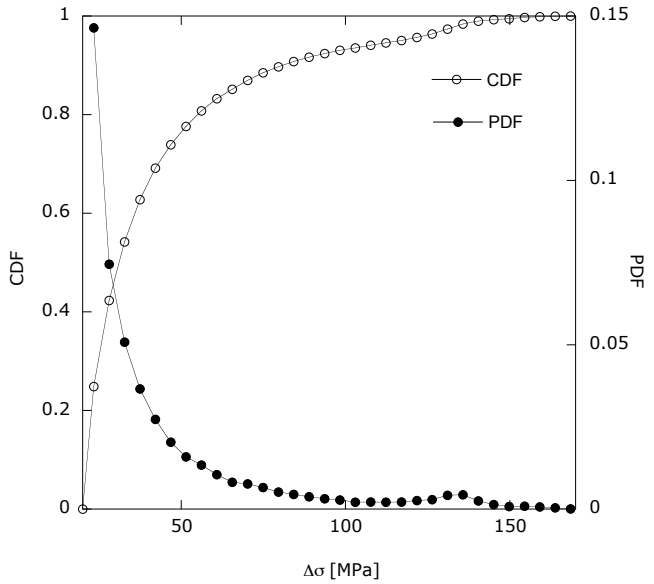

Fig. 6 Empirical cumulative density function and corresponding probability density function of the stress range.

The stress range process $\{\Delta\sigma(N)\}$ is modelled as a stationary process with autocovariance function according to Eq. (15). Information on the correlation structure during service is not available. Instead, various values of the correlation length z are applied, to study the influence of this parameter on the reliability.

5.2 EXAMPLES OF LOAD SEQUENCES

To illustrate the influence of the correlation length z on the stress range process $\{\Delta\sigma(N)\}$, Fig. (7a-d) show random realizations of $\{\Delta\sigma(N)\}$ for varying z. The sequences shown here are obtained by fixing the initial values of the stress range at values $\Delta\sigma_1 = 20,\ 30,\ 146$ MPa. For correlation lengths $z \leq 10^5$, the initial value does not influence the general shape of the load sequence. When the correlation length is of the same order of magnitude as the service life ($z = 10^7$), the initial value can influence the shape of the load sequence, which shows slowly varying stress range levels.

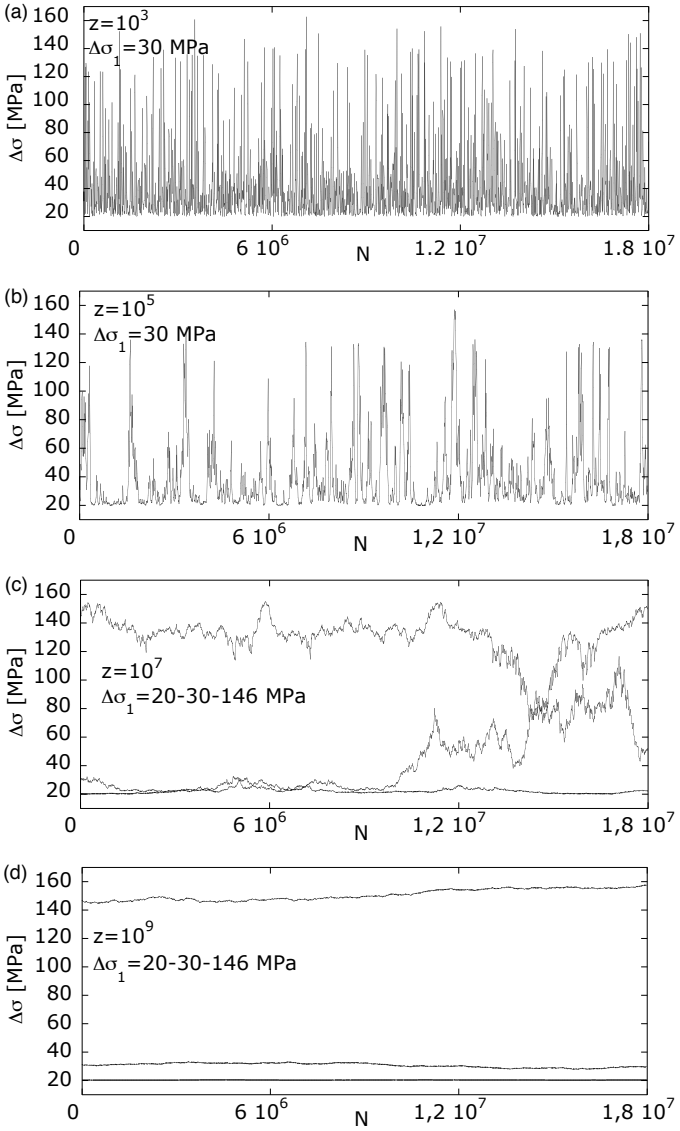

Fig. 7 Random load sequences obtained starting from three different values of initial stress, $\Delta\sigma_1 = 20, 30, 146\ MPa$, and applying various correlation lengths: $z = 10^3$ (a), $z = 10^5$ (b), $z = 10^7$ (c), $z = 10^9$ (d).

Load sequences obtained with $z \approx 10^7$ might be used to simulate a situation where the components undergo only a few different mission types during their service life. For correlation length significantly higher than the service life of the component ($z \approx 10^9$), the load is approximately constant. In this case, the random process model might be replaced by a random variable model.

5.3 RESULTS

The influence of the correlation length z on the probability of failure is assessed by fixing the block length at $\Delta N = 10^3$ and varying z. To study the influence of the initial flaw size distribution, the evaluation is carried out for two different POD curves, as shown in Fig. (2). Additionally it is conservatively assumed that one flaw is present in each component.

Figs. (8a) and (8b) show the probability of failure p_F evaluated with the subset simulation, plotted against z for the POD curves. As a reference, results obtained with Monte Carlo simulation (MCS) are also reported with their 95% confidence interval. The evaluation for $z > 10^9$ is carried out with MCS describing the load as a random variable.

The results obtained with subset simulation are consistent with MCS results. Even if the probabilities of failure are quite high in the examples presented here, subset simulation still leads to shorter computation times. For example, to obtain the results for $z = 1$ in Fig. 9a, the evaluation with Monte Carlo is around ten times longer than with Subset.

The probability of failure is not affected by changes in the correlation length z for values of $z < 10^4$. For higher values of z, the probability of failure increases with increasing z until it reaches a maximum for values of z close to the service life time, around $10^6 - 10^7$. For $z > 10^7$, p_F decreases again until it reaches the value corresponding to the random variable case ($z = \infty$).

Values of z in the range $10^6 - 10^7$ correspond to cases with a few distinct service conditions during the service life. These are the most unfavourable cases, since they imply a high probability of enduring a high load level during an extended time period. Shorter correlation lengths correspond to a single service condition with randomly varying stress ranges. In these cases, lower failure probabilities are observed because the mixing of the stress ranges decreases the actual uncertainty in the loading (law of large numbers). Finally, for $z > 10^7$, the probability of having a high load level during lifetime decreases, and therefore the probability of failure decreases.

By comparing the probability of failure obtained for two different POD curves (Figs. 8a and 8b), it can be noticed that p_F is sensitive to the distribution of the initial flaw size in the case of low correlation lengths. For higher correlation lengths, the probability of failure is less influenced by the initial flaw size.

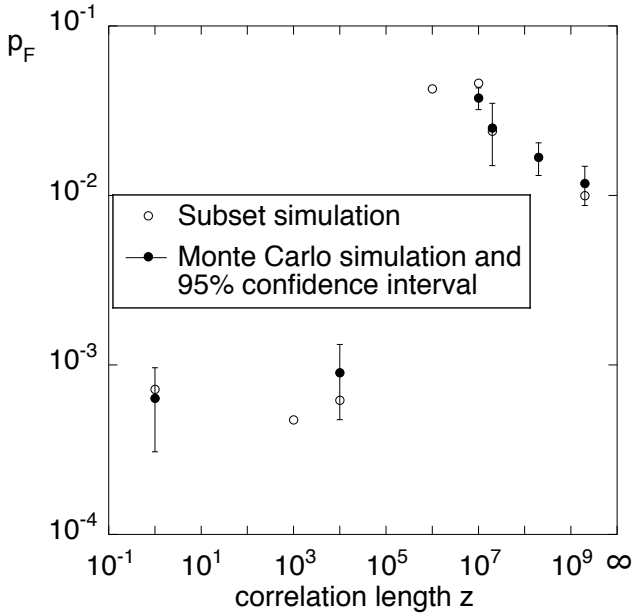

Fig. 8a Probability of failure versus correlation length for the initial flaw size distribution reported in Fig. 2a.

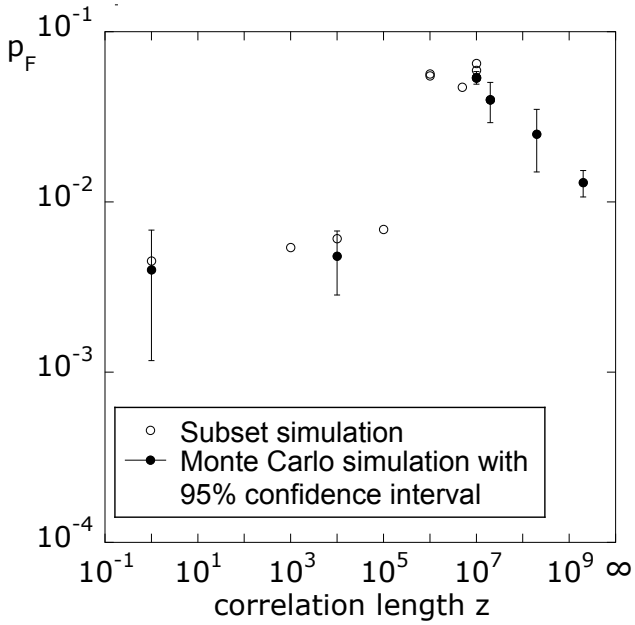

Fig. 8b Probability of failure versus correlation length for the initial flaw size distribution reported in Fig. 2b.

6 CONCLUSIONS

The probability of failure of mechanical components subjected to fatigue, with a service life of around 10^7 stress cycles, is evaluated using the subset simulation method and a fatigue crack growth algorithm based on the Forman-Mettu equation. Random processes with varying correlation lengths are applied to describe various types of fatigue loading, corresponding to different mission types. The results show that the probability of failure is strongly influenced by the characteristics of the stress process beyond the marginal distribution of stress ranges (the load spectrum). The probability of failure appears to be particularly high for stress range processes with correlation lengths slightly shorter than the service life.

7 ACKNOWLEDGMENTS

The support of Iason Papaioannou in the implementation of the subset simulation is gratefully acknowledged. Dr Mario Rossi, director of Tenaris R&D center, is kindly acknowledged for the permission to publish this paper.

REFERENCES

1. 2002, EN13445-3, Unfired pressure vessels – Design
2. 2005, EN 1993-1-9, Eurocode 3: Design of steel structures – Fatigue
3. 2005, BS7910, Guide to methods for assessing the acceptability of flaws in metallic structures
4. FORMAN R.G. METTU S.R., 1992, 'Behavior of surface and corner cracks subjected to tensile and bending loads in a Ti–6Al–4V alloy', *in: H.A. Ernst, A. Saxena, D.L. McDowell (Eds.), Fracture Mechanics: Twenty-Second Symposium, ASTM STP 1131, vol. I, American Society for Testing and Materials, Philadelphia, pp. 519–546*
5. BECK A.T. MELCHERS R.E., 2004, Overload failure of structural components under random crack propagation and loading – a random process approach', *Structural Safety, Vol. 26, pp. 471–488*
6. YANG J.N. MANNING S. D., 1996, 'A simple second order approximation for stochastic crack growth analysis', *Engineering Fracture Mechanics Vol. 53, No. 5, pp. 677-686.*
7. MALJAARS J. STEENBERGEN H.M.G.M. VROUNWENVELDER A.C.W.M., 2018, 'Probabilistic model for fatigue crack growth and fracture of welded joints in civil engineering structures', *International Journal of Fatigue Vol. 38, pp. 108-177*
8. HEULER P, KLAÜTSCHKE H., 2005 'Generation and use of standardised load spectra and load time histories.' *International Journal of Fatigue, Vol. 27, No.8, pp. 974–990.*
9. DOMINGUEZ J., ZAPATERO J., PASCUAL J., 1997 'Effect of load histories on scatter of fatigue crack growth in aluminium alloy 2024 – T351 ', *Engineering Fracture Mechanics, Vol. 56, No.1, 65-76.*
10. LIN Y. K. YANG J. N., 1985, A stochasti theory of fatigue crack propagation', *AIAA Journal, Vol. 23, No. 1,pp. 177-124.*
11. MATTRAND C., BOURINET J. M., 2011, 'Random load sequences and stochastic crack growth based on measured load data', *Engineering Fracture Mechanics, Vol. 78, pp. 3030-3048.*
12. RYCHLIK I., 1996, 'Simulation of load sequences from rainflow matrices: Markov method', *International Journal of Fatigue, Vol. 18, No. 7, pp. 429-438.*
13. STRAUB D., 2009 'Stochastic modeling of deterioration processes through dynamic Bayesian networks', J*ournal of Engineering Mechanics, Trans. ASCE, 135(10), 1089-1099.*
14. AU S.K., BECK J.L., 2001, 'Estimation of small failure probabilities in high dimensions by subset simulations', *Probabilistic Engineering Mechanics, Vol. 16, pp. 263-277.*
15. HARTER J. A., 2006, AFGROW 'Users guide and technical manual', US air force research laboratory technical report AFRL-

VA-WP-TR-2006-XXXX, Air vehicle directorate, 2790 D Street, Ste 504.
16. CRISTEA M.E., BERETTA S., ALTAMURA A., 2012,'Fatigue limit assessment on seamless tubes in presence of inhomogeneities: experimental small vs. full scale testing', *International Journal of Fatigue, Vol. 41, pp. 150-157.*
17. ALTAMURA A, BERETTA S., 2011, 'Reliability assessment of hydraulic cylinders considering service loads and flaw distribution' submitted to *International Journal of Pressure Vessels and Pipings*.
18. ALTAMURA A., BERETTA S., DESIMONE H. J., 2009, Reliability of hydraulic cylinders, *Proceeding of the International Conference on Fracture ICF12, Ottawa*.
19. NEWMAN, 1984, 'A crack opening stress equation for fatigue crack growth', *International Journal of Fracture, Vol. 24, pp. 131-135*.
20. ANDERSON T., 1995 'Fracture mechanics: fundamentals and applications', *CRC Press, Boca Raton*
21. NEWMAN J. C., RAJU J. S., 1986,'Stress Intensity Factor Equations for Cracks in Three-Dimensional Bodies Subjected to Tension and Bending Loads' *in 'Computational methods in the mechanics of fracture, Elsevier Science.*
22. HONG H. P., 1997, 'Reliability analysis with non destructive inspection', *Structural Safety, Vol. 19, No. 4, pp. 383-395.*
23. ZERBST U., SCHÖDEL M., WEBSTER S., AINSWORTH R., 2007, 'Fitness-for-service Fracture assessment of structures containing cracks, Elsevier Science.
24. VANMARCKE EH., 1983, Random fields. Analysis and synthesis. Cambridge', *MA: MIT Press.*
25. HOHENBICHLER M., RACKWITZ R., 1981, 'Non-normal dependent vectors in structural safety', *Journal of Engineering Mechanics, Vol. 107, No. 6, pp. 1227-1238.*
26. RACKWITZ R. FIESSLER B., 1978, 'Structural Reliability under Combined Random Load Sequences', *Computers and Structures , Vol. 9, pp. 484-494.*